AJNR

Focal Brain Glucose Hypometabolism in Patients with Neuropsychologic Deficits after Diffuse Axonal Injury

T. Nakashima, N. Nakayama, K. Miwa, A. Okumura, A. Soeda and T. Iwama

AJNR Am J Neuroradiol 2007, 28 (2) 236-242
http://www.ajnr.org/content/28/2/236

ORIGINAL RESEARCH

Focal Brain Glucose Hypometabolism in Patients with Neuropsychologic Deficits after Diffuse Axonal Injury

T. Nakashima
N. Nakayama
K. Miwa
A. Okumura
A. Soeda
T. Iwama

BACKGROUND AND PURPOSE: Neuropsychologic deficits are well-known sequelae of traumatic brain injury. However, the cerebral correlates of these deficits are still unclear. The aim of the present study was to elucidate the regions of cerebral dysfunction correlated with such neuropsychologic deficits after traumatic brain injury.

METHODS: Sets of fluorine-18 fluorodeoxyglucose–positron-emission tomography (FDG-PET) images in the resting state were obtained from 12 patients with neuropsychologic deficits after diffuse axonal injury and from 32 healthy volunteers. The cortical metabolic activity of each subject's PET image sets was extracted using 3D stereotactic surface projection (3D-SSP). A "normal" data base was created using the extracted datasets of the healthy subjects. The patients' datasets were compared with the normal data base by calculating a statistical *Z*-score on a pixel-by-pixel basis in searches for focal metabolic abnormalities.

RESULTS: Group comparisons revealed hypometabolism in the cingulate gyrus with additional involvement of the lingual gyrus and cuneus. Individual case-by-case analyses disclosed differences in the site and extent of the hypometabolism in the cingulate gyrus of each case. Predominant hypometabolism was found in the anterior cingulate gyrus of 6 patients, the middle cingulate gyrus of 2 patients, and the posterior cingulate gyrus of 4 patients.

CONCLUSION: Interpretation of FDG-PET using 3D-SSP facilitates the identification of regional hypometabolism in the cerebral cortex of patients after diffuse axonal injury. Dysfunction of the cingulate gyrus, lingual gyrus, and cuneus may play a crucial role in neuropsychologic deficits after traumatic brain injury.

Neuropsychologic deficits are well-known sequelae of traumatic brain injury (TBI). The deficits represent a complex combination of cognitive impairments and behavioral disorders and often become substantial sources of morbidity for affected persons.[1,2] However, neither the underlying mechanisms nor the cerebral correlates of the deficits are clearly understood.

Several studies have been carried out to determine the regional cerebral dysfunction responsible for such deficits[3] using functional brain imaging, such as single-photon emission CT (SPECT)[4-6] or positron-emission tomography (PET),[7-9] which has the potential to reveal cerebral dysfunction in regions without any detectable structural lesions on CT or MR imaging.[10] Fluorine-18 fluorodeoxyglucose–PET (FDG-PET) is the only established technique that can evaluate cerebral glucose metabolism in vivo. Based on the principle that regional glucose metabolism reflects the neuronal activity of the region, focal hypometabolism indicates an area of neuronal dysfunction. Therefore, FDG-PET has an advantage for elucidating focal brain dysfunction compared with the cerebral perfusion image obtained by SPECT. However, few studies have used FDG-PET to explore the lesions correlated with neuropsychologic deficits after TBI.[7-9]

Received January 31, 2006; accepted after revision April 4.

From the Department of Neurosurgery (T.N., N.N., K.M., A.O.), Chubu Ryogo Center, Kizawa Memorial Hospital; and Department of Neurosurgery (A.S., T.I.), Graduate School of Medicine, Gifu University.

This study was supported in part by grants from Japanese Ministry of Health, Labor and Welfare.

Address correspondence to Toshihiko Nakashima, MD, Department of Neurosurgery, Chubu Ryogo Center, Kizawa Memorial Hospital, 630 Shimokobi, Kobi-cho, Minokamo, Gifu, 505-0034, Japan; e-mail: torinaka@quartz.ocn.ne.jp

For the analysis of PET images, the region of interest (ROI) method has been widely used. However, problems are associated with this method, such as poor objectivity and low reproducibility of the results. Therefore, interpretation of PET images using stereotactic brain coordinate systems, such as 3D stereotactic surface projections (3D-SSP)[11-13] and statistical parametric mapping (SPM),[14,15] would allow greater consistency in the reported results and make it easy to determine the spatial extent of the abnormal site on the brain map. However, there is a small difference between the 2 methods. In particular, 3D-SSP is used as a clinical application for diagnosis by detecting the distribution forms of abnormal regions on the brain surface, whereas SPM aims to indicate foci with a significant difference over the whole brain. Furthermore, 3D-SSP is programmed to avoid the effect of brain atrophy, such that the results are less affected by regional brain atrophy than SPM, even in a single case-by-case analysis.

Previous analyses of FDG-PET using 3D-SSP successfully demonstrated subtle decreases in glucose metabolism in the region of the posterior cingulate cortex and the cinguloparietal transitional area in patients with Alzheimer disease at a very early stage.[16] Following this methodology, the present study was conducted to elucidate local metabolic reduction in patients after TBI, which may correlate with neuropsychologic deficits.

Methods

Patients and Healthy Subjects

Twelve patients (8 men and 4 women) with neuropsychologic deficits after diffuse axonal injury (DAI) were recruited from the Department of Neurosurgery in Kizawa Memorial Hospital between 2002 and

2004. The recruitment was part of an ongoing cross-sectional study of neuropsychologic deficits (A model project for supporting persons with higher brain dysfunction; Japanese Ministry of Health, Labor and Welfare), and the 12 patients were drawn from a larger group of 31 patients with neuropsychologic deficits after TBI or cerebrovascular accidents. Despite making a good recovery after TBI, the impairment of memory, attention, and executive function caused them to become unemployed. When probing the functional consequences of damages to the brain, the heterogeneity of the pathogenesis of brain injury may represent a reason for the failure to find consistent relationships between the localization of lesions and neuropsychologic deficits after TBI. Simplifying the pathogenesis and eliminating the effect of focal injury in cerebral cortex, which had negative correlation with neuropsychologic deficits, the following inclusion criteria were made: moderate or severe injury,[17] diffuse injury type II or III according to the CT classification,[18] and no physical handicaps. At the time of the FDG-PET study, the mean age of the patients was 30.4 years (range, 18–50 years). The mean time since injury was 28.8 months (range, 3–71 months). Initial CT scans after injury showed subarachnoid hemorrhage or intraventricular hemorrhage without diffuse brain swelling in 9 of 12 patients. Three of 12 patients showed diffuse brain swelling with midline shift under 5 mm. No focal injury with volume exceeding 25 mL was demonstrated in the patients. A small mixed-attenuation area suggesting cerebral contusion was shown in 5 of 12 patients. Three of the cerebral contusions were present in the right frontal lobe and 2 of them were in the right temporal lobe. The patients and their families were informed of the experimental aim of the study and gave their consent to participate.

The cognitive impairments of the patients were diagnosed by administering the following battery of neuropsychologic tests: memory was assessed using the Wechsler Memory Scale, Revised Edition (WMS-R); attention was assessed using the Paced Auditory Serial Attention Task (PASAT) and D-CAT (similar to Ruff's 7 series, normalized by more than 350 normal subjects); executive function was assessed using the Wisconsin Card Sorting Test (WCST); and general intelligence was assessed using the Wechsler Adult Intellectual Scale, Revised Edition (WAIS-R). The numbers of patients showing deficit on each cognitive domain were as follows: 9 of 10 patients tested by WMS-R showed a positive memory problem, 10 of 11 patients tested by PASAT and/or D-CAT showed an attention problem, and 5 of 7 patients tested by WCST showed an executive function problem. Four of 12 patients were asymptomatic, and 8 patients had a subnormal score on the intelligence quotient (IQ).

The age-similar healthy subjects were 32 volunteers with no prior history of head injury who were recruited by advertising. The healthy subjects were divided into 2 age-similar groups, designated the data base group (DBG) and the control group (CG), in a random fashion. The DBG and CG consisted of 20 subjects (average age, 35.6 years; range, 21–50 years) and 12 subjects (average age, 35.5 years; range, 22–50 years), respectively. The PET image datasets of the DBG were used to create a data base of 3D-SSP. The datasets of the CG were analyzed in the same way as those of the patients to validate the reliability of the created data base and the result of 3D-SSP analyses.

Magnetic Resonance Imaging

MR images were obtained for all the patients and healthy subjects using a 1.5T scanner (Signa; GE Healthcare, Milwaukee, Wis). The imaging protocol consisted of 3 imaging sessions of the same geometry (15 sections; axial plane; section thickness, 6 mm; section gap, 3 mm): 1) T1-weighted fast spin-echo (TR, 350 ms; TE, 10 ms; FOV, 25 cm; data matrix, 256 × 224); 2) axial T2-weighted fast spin-echo (TR, 2600 ms; TE, 100 ms; FOV, 25 cm; data matrix, 256 × 224); and 3) gradient-echo echo-planar imaging (TR, 1000 ms; TE, 12 ms; FOV, 25 cm; data matrix, 256 × 224; flip angle, 20°).

Positron-Emission Tomography

Resting-state measurement of glucose metabolism with ^{18}F-FDG-PET was performed as follows. The PET scans were performed using an Advance scanner (GE Healthcare) that provided 35 transaxial images at 4.25-mm intervals. Patients and healthy subjects fasted for at least 4 hours before the scanning. After intravenous administration of 5.3 MBq/kg ^{18}F-FDG, the subjects were kept in a dimly lit isolation room and instructed to remain still with their eyes open to avoid falling asleep. A set of transaxial images was obtained with a standard 2D emission scan mode starting 40 minutes after the injection. Thereafter, a transmission scan was performed for attenuation correction.

Data Analysis

PET image analysis with 3D-SSP was performed using the Neurostat software established by Minoshima et al.[13] Each image set was realigned to the bicommissural stereotactic coordinate system. The differences among individual brain sizes were removed by linear scaling, and regional anatomic differences were minimized by a nonlinear warping technique.[19] As a result, each brain was standardized anatomically to match with a standard atlas of the brain[20] while preserving the regional metabolic activity. Thereafter, the maximum cortical activity was extracted to adjacent predefined surface pixels on a pixel-by-pixel basis using the 3D-SSP technique.[13] This cortical data extraction technique compensates for small anatomic differences in the gray matter structures (such as variable depth of the gyri) across patients and minimizes the partial volume of the white matter. Approximately 16,000 predefined surface pixels covered the entire cortex, including the medial aspect of the 2 hemispheres. The extracted data for the cortical activity were normalized according to the mean global activity before further analyses.

Individual case-by-case analyses were performed as follows. A normal reference data base was created by calculating the mean and SD of the activity for each surface pixel using the normalized datasets of the DBG subjects. Thereafter, the normalized activity of each patient and CG subject was compared with the normal reference data base by a *Z*-score (Z = [normal mean value] − [individual value]/normal SD). A positive *Z*-score represented a reduced metabolic activity. To confirm the characteristic metabolic pattern of the patients, 2-sample Student *t* test values were calculated on a pixel-by-pixel basis between the patient group and the DBG. Next, the calculated *t* values were transformed to *Z*-scores by a probability integral transformation. The *Z*-score data were then displayed on the 3D-SSP brain surface map for visual inspection.

Individual 3D-SSP brain surface maps of each patient and CG subject were evaluated by an expert reader who was blind to the clinical data. The locations of hypometabolism were also evaluated by a stereotactic extraction estimation method (SEE) established by Mizumura et al[21] to minimize the subjective bias and variability on visual inspection. In brief, the 3D-SSP brain surface map was divided into 64 gyrus-level segments according to the Talairach Daemon brain atlas (Talairach Daemon; Research Imaging Center, University of Texas Laboratory).[22,23] Next, the proportion of surface pixels with *Z* values over a threshold value (this study used $Z = 2$ as the threshold) was calculated in each respective segment and expressed as the "extent" of the lesion in each gyrus-level segment.

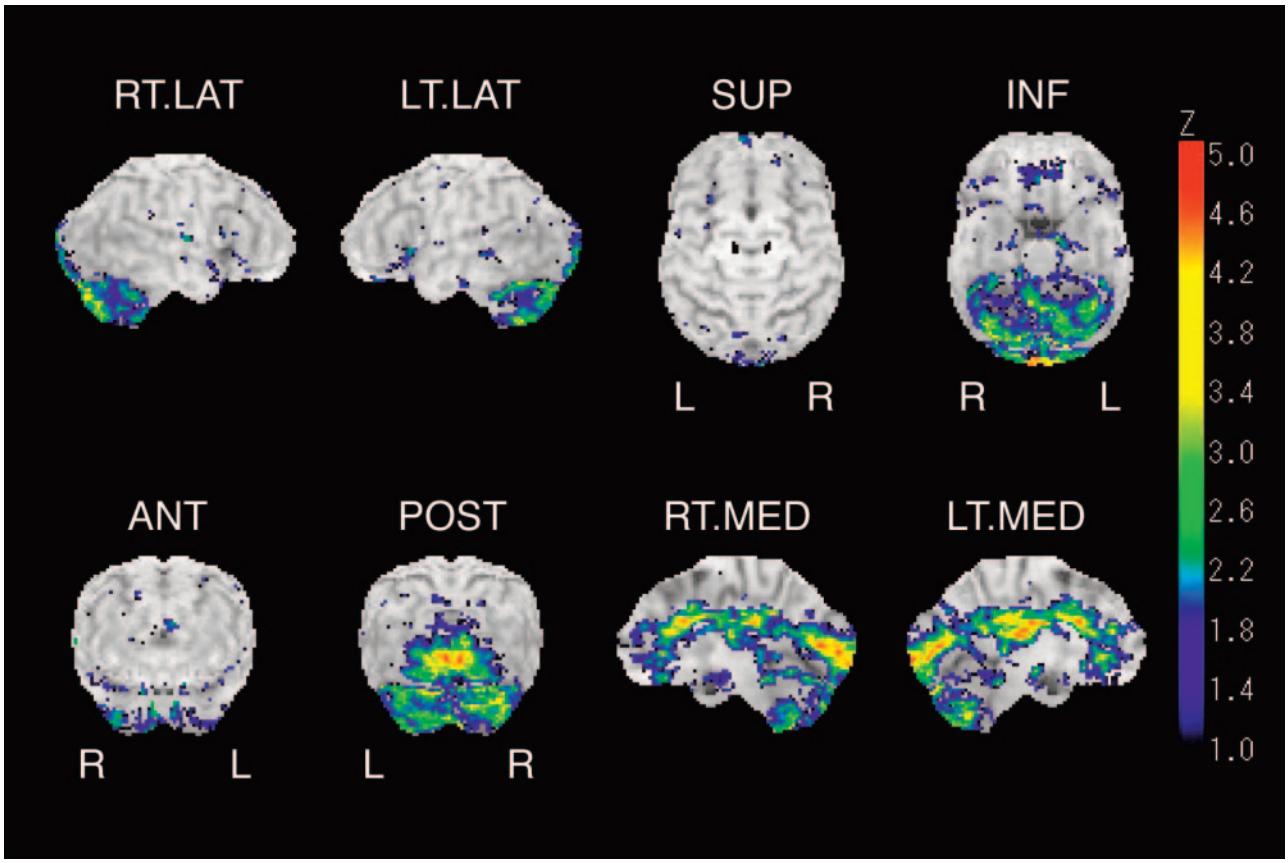

Fig 1. *Z*-score brain surface map represents areas of metabolic reduction in patients in comparison with healthy subjects (data base group). Right lateral (*R.LAT*), left lateral (*L. LAT*), superior (*SUP*), inferior (*INF*), anterior (*ANT*), posterior (*POST*), right medial (*R. MED*), and left medial (*L. MED*) views are shown. Reduction of glucose metabolism is evident in medial aspects of cerebrum especially in cingulate gyrus, lingual gyrus, and cuneus.

Results

Brain MR imaging revealed neither anomalies nor prior pathologic changes in any of the healthy subjects. Traces of cerebral contusion were found in the frontal or temporal lobes of 5 patients. A few scattered hemosiderin deposits in the cerebral white matter, suggesting the presence of microbleeding in the acute stage of DAI, were observed in 5 patients. The area of cerebral contusion was shown as the focus of glucose hypometabolism on the axial view of the PET images, as well as on the 3D-SSP brain surface map. However, none of the local hypometabolism shown on the axial view of the PET image coincided with the hemosiderin deposit demonstrated by MR imaging.

Group comparisons between the patient group and the DBG clearly revealed areas of decreased cortical glucose metabolism on the 3D-SSP brain surface map. Local hypometabolism was identified in the anterior, middle, and posterior cingulate gyrus, lingual gyrus, cuneus, and cerebellum on visual inspection. The hypometabolism was mostly observed on the medial aspect of the bilateral cerebral hemisphere with a symmetric pattern (Fig 1). The "extent" (proportion of surface pixels with a *Z* score >2) of representative gyrus level segment is shown in Table 1. When significant hypometabolism in a segment was defined as exceeding 30%, the anterior, middle, and posterior cingulate gyri, lingual gyrus, cuneus, and right thalamus could be evaluated for their hypometabolic regions. On the contrary, group comparisons between the CG and the DBG revealed no significant hypometabolic regions (Fig 2).

Table 1: Abstract from the stereotactic extraction estimation (SEE) results of group comparison

Gyrus Level Classification	Total Projection	Projection ($Z > 2$)	Extent Ratio (%)
Anterior cingulate gyrus			
Left	180	94	52.2
Right	180	85	47.2
Middle cingulate gyrus			
Left	267	118	44.2
Right	267	94	35.2
Posterior cingulate gyrus			
Left	98	58	59.2
Right	98	43	43.9
Lingual gyrus			
Left	100	89	89.0
Right	99	91	91.9
Cuneus			
Left	306	119	38.9
Right	303	127	41.9

Note:—In each row, anatomic information, total coordinates, number of coordinates showing abnormalities ($Z > 2$), and proportion of abnormal pixels in total surface pixels are presented from the left. Table shows the results of representative gyrus level segments extracted from 32 segments of whole cerebral surface.

The proportion of surface pixels with a *Z* score >2 was only 2.4% of the total surface pixels of the cerebrum.

Individual case-by-case analyses also revealed local hypometabolism in the cingulate gyrus, lingual gyrus, and cuneus. However, the distribution of hypometabolic region was different in each individual case (Fig 3). Patterns of cortical metabolic abnormalities in the medial surface of cerebral hemi-

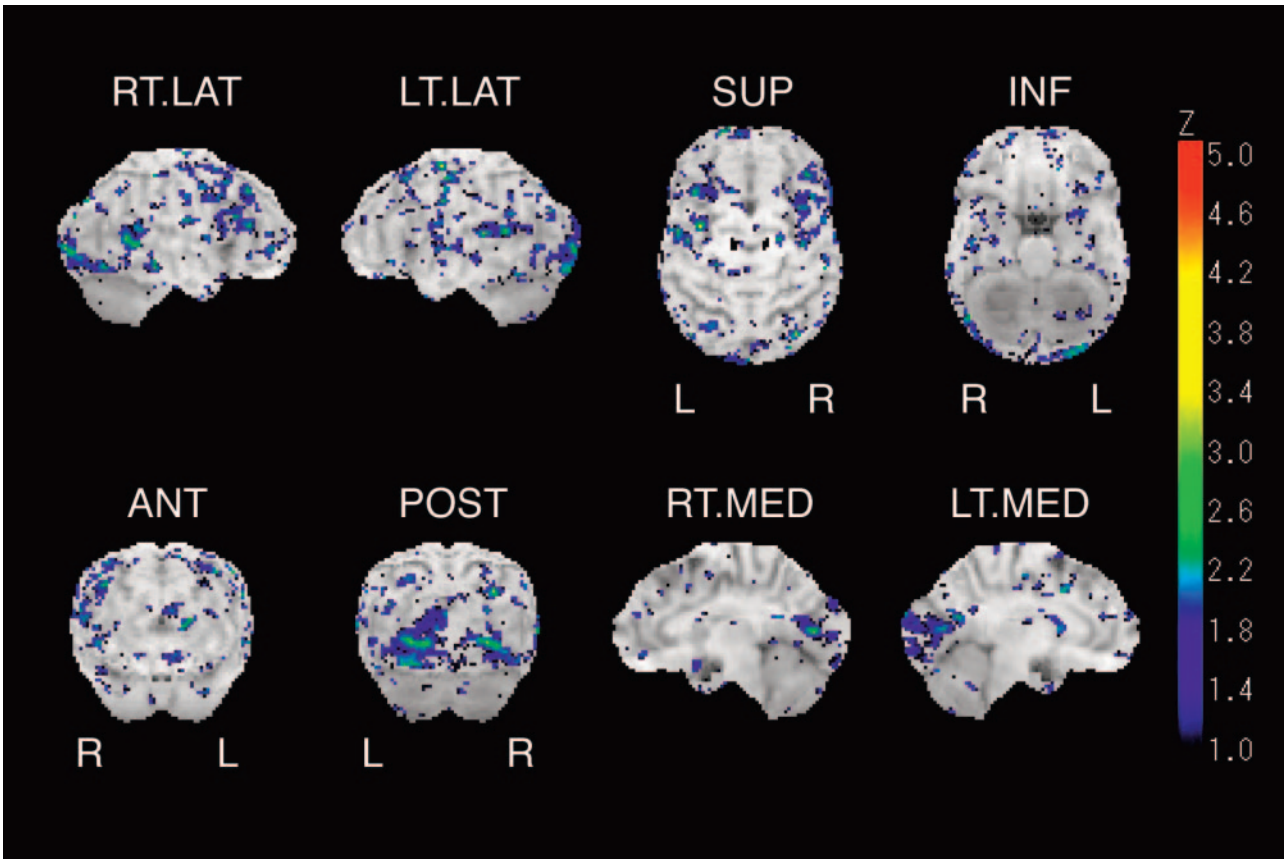

Fig 2. *Z*-score brain surface map represents the result of group comparison between 2 healthy subjects groups such as control group (CG) and data base group (DBG). Right lateral (*R.LAT*), left lateral (*L. LAT*), superior (*SUP*), inferior (*INF*), anterior (*ANT*), posterior (*POST*), right medial (*R. MED*), and left medial (*L. MED*) views are shown. Marked metabolic reduction is not shown on the medial surface of cerebrum.

sphere were examined for discriminating the patients from normal control subjects. Visual inspection resulted in 2 false-negative cases in the patient group and no false-positive cases in CG subjects. In the false-negative cases, clusters of the pixels showing high *Z* score in the middle and posterior cingulate gyrus were so small that the images were not assessed as abnormal. Every image showing the metabolic reduction in the anterior cingulate gyrus (case 1–6; Table 2) was identified as abnormal.

Estimation of the individual *Z*-score data disclosed that the "extent" (proportion of the surface pixels with a *Z* score >2) of the hypometabolism in regions of the anterior, middle, or posterior cingulate gyrus of individual patients was significantly higher than that of individual CG subjects. The "extent" revealed hypometabolism of the lingual gyrus and cuneus in 5 patients in the unilateral or bilateral cerebral hemisphere (Table 2). Regarding the spatial distribution of the hypometabolism in the cingulate gyrus, the 3D-SSP brain surface map facilitated the visualization of differences among the patients (Fig 2). The "extent" disclosed a predominant hypometabolism in the anterior cingulate gyrus in 6 patients, middle cingulate gyrus in 2 patients, and posterior cingulate gyrus in 4 patients (Table 2). Three of 4 patients showing predominant hypometabolism in the posterior cingulate gyrus revealed a concomitant metabolic reduction in the lingual gyrus and cuneus, whereas metabolic reduction in the lingual gyrus and cuneus was found in only 2 of 8 patients showing predominant hypometabolism in the anterior or middle cingulate gyrus (Table 2).

Hypometabolism of the cerebellar cortex was demonstrated not only by the group comparisons but also by the individual case-by-case analyses. However, the SEE software did not support *Z*-score estimation for the cerebellar cortex; therefore, the assessment of metabolic reduction in the cerebellar cortex was based simply on visual inspection.

Discussion

Interpretation of FDG-PET by 3D-SSP facilitated the visualization and evaluation of regional hypometabolism, compared with previous neuroimaging studies of the patients with neuropsychologic deficits after TBI. To account for the metabolic reduction, the following 2 main mechanisms have been proposed: 1) local neuronal loss and 2) decreased neuronal activity as a result of deafferentation. In the present study, MR imaging did not reveal focal structural damage to the cingulate cortex or the other cortices in which hypometabolism was demonstrated by the group comparison. Therefore, the regional metabolic reduction in the cingulate gyrus, lingual gyrus, and cuneus is suggested to arise as a result of deafferentation of the neurons[24] interconnecting the hypometabolic regions with other parts of the cerebrum.

There is now evidence that the anterior cingulate cortex has extensive reciprocal connections with the prefrontal, parietal, and temporal cortices as well as with the limbic and reticular

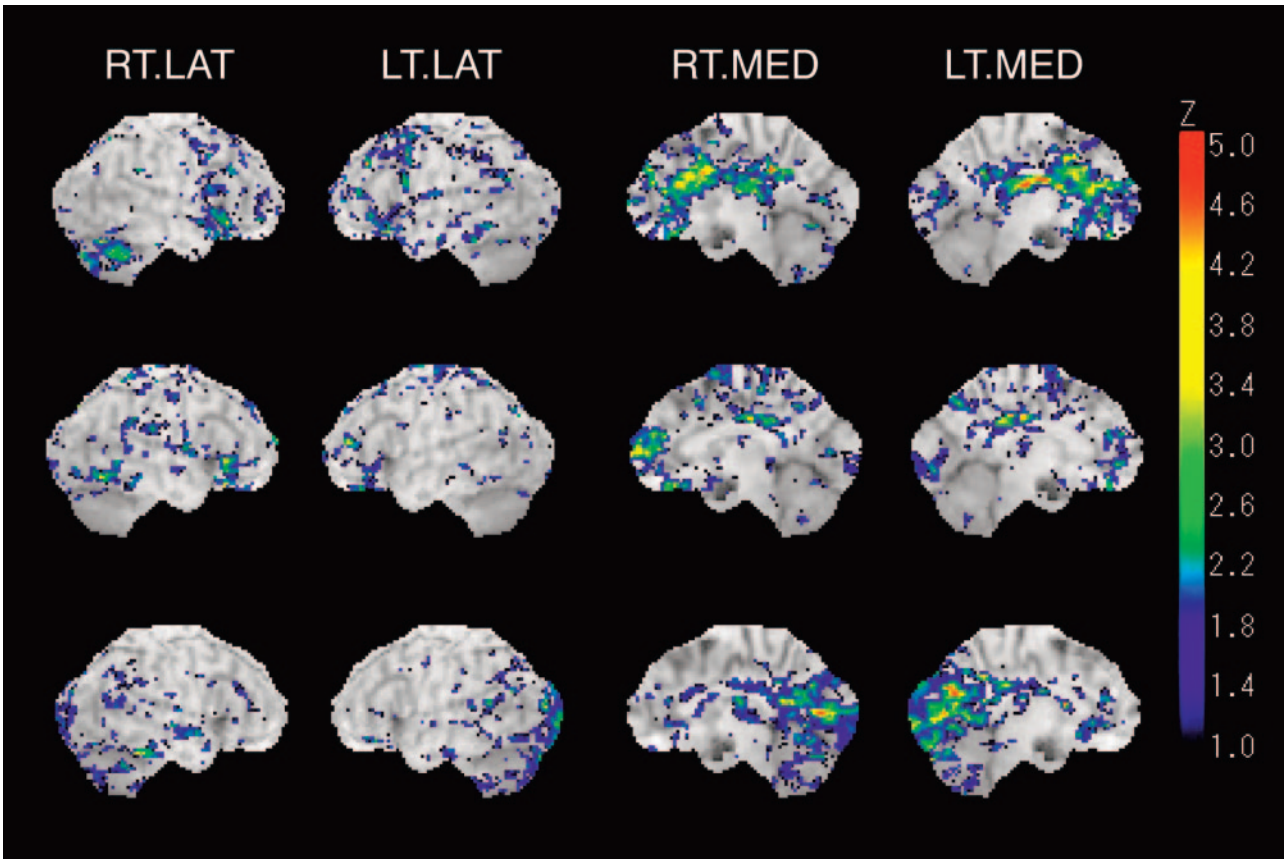

Fig 3. *Z*-score brain surface map of representative cases shows a prominent metabolic reduction on respective gyrus level segment in cingulate gyrus.

Top, 46-year-old man (case 4) shows hypometabolism in anterior cingulate gyrus.

Middle, 38-year-old woman (case 7) shows hypometabolism in middle cingulate gyrus. Metabolic reduction shown in the right frontal lobe is the result of cerebral contusion.

Bottom, 28-year-old man (case 12) shows hypometabolism in posterior cingulate gyrus with concomitant hypometabolism of lingual gyrus and cuneus.

Table 2: Proportion of surface pixels showing abnormalities ($Z > 2$) in each case

		Anterior Cingulate Gyrus		Middle Cingulate Gyrus		Posterior Cingulate Gyrus		Lingual Gyrus	
Case No.	Age & Sex	Right	Left	Right	Left	Right	Left	Right	Left
1	26 F	37.8	58.9	9.0	2.6	2.0	0.0	0.0	0.0
2	39 M	20.0	15.6	9.7	11.2	2.0	0.0	6.1	25.0
3	50 M	34.4	32.8	29.2	38.2	2.0	1.0	0.0	3.0
4	46 M	45.6	48.9	32.2	24.7	10.2	8.2	0.0	2.0
5	24 F	57.2	46.1	9.7	3.0	7.1	5.1	34.3	33.0
6	22 M	57.8	37.8	6.0	4.5	4.1	24.5	35.4	52.0
7	38 F	1.1	2.8	11.2	13.9	2.0	1.0	0.0	16.0
8	23 M	1.7	5.6	16.1	15.4	1.0	1.0	0.0	33.0
9	22 M	1.1	0.0	1.1	1.9	16.3	21.4	17.2	21.0
10	44 F	0.0	0.0	2.6	2.6	53.1	6.1	69.7	6.0
11	19 M	1.7	0.6	5.2	1.9	3.1	11.2	72.7	72.0
12	28 M	2.2	7.8	2.2	6.7	42.9	43.9	23.2	61.0
CG	Mean	2.3	1.8	0.9	1.9	0.9	2.5	6.5	9.9
	SD	2.8	2.8	0.9	2.4	2.0	4.2	11.9	17.4

Note:—CG indicates control group.

systems. It has been proved to play a crucial role in the expression of frontal lobe functions and is believed to form the central part of an executive/attentional system and to play a key role in cognition.[25] The posterior cingulate cortex also has various reciprocal connections with the limbic system and association cortices,[26,27] such as the temporal and parietal cortices distinct from those of the anterior cingulate cortex.[28] It has been proved to play an important role in learning and memory function. The lingual gyrus and cuneus have been believed to mediate the neural function of visual perception in cooperation with the functionally conjunctive occipitotemporal cortex.[29,30] Histopathologic study has shown widespread axonotomy in cerebral white matter of the patients after DAI.[31] Deafferentation caused by the axonotomy to the neurons interconnecting cingulate gyrus with other cerebral cortices of bilateral hemisphere may result in the symmetrical metabolic

reduction of the cingulate gyrus. The dysfunction of bilateral cingulate cortex produced by the axonotomy may be the fundamental mechanism of the neuropsychologic deficits after DAI.

The ventral anterior and posterior cingulate cortices have been proved to show greater activities in the resting state than during cognitive tasks. Based on this phenomenon, the following hypothesis has been proposed.[32,33] The posterior cingulate cortex has significant functional connectivity with the ventral anterior cingulate, prefrontal, and other cerebral cortices that constitute a default mode network active during the resting state. They integrate cognitive and emotional processing when tasks with a high cognitive demand cue such processing. Because the FDG-PET images in the present study were obtained in the resting state, the metabolic reduction shown in the cingulate cortex of the patients might indicate a dysfunction of the default mode network, which might be involved in the pathogenesis of the neuropsychologic deficits.

The results of this study showing local glucose hypometabolism in the cingulate gyrus are in agreement with previous research by Fontaine et al[9] who quantitatively analyzed the cerebral glucose metabolism of patients with neuropsychologic deficits after severe TBI using the ROI method. They showed significant correlations between the cingulate gyrus metabolism and cognitive functions. At the same time, they also demonstrated significant metabolic reduction in the bilateral prefrontal cortices. Although prefrontal dysfunction has been suspected of contributing to the neuropsychologic deficits after TBI, the present study revealed no metabolic reduction in the prefrontal cortex. This discrepancy may depend on the differences in the methodologies used for the analyses. The cortical activity was extracted and analyzed in the present study; however, subcortical activity may be included by the measurement using the ROI method.

This is the first study to demonstrate the hypometabolism in the lingual gyrus and cuneus in patients with neuropsychologic deficits after DAI. The results indicate that the dysfunction of the lingual gyrus and cuneus may correlate with the deficits in visual perception of the patients.[29,30] However, it should be noted that the metabolic activities of the lingual gyrus and cuneus of the present study varied to some extent even in the control subjects. The value of the SD for the "extent" in the lingual gyrus and cuneus was larger than that of the cingulate gyrus in the control group. This may depend on the variable neuronal activation in the visual and visual association cortices during the uptake period of FDG. Although the subjects were kept in a dimly lit room after the FDG injection, they did not close their eyes. Therefore, further studies are needed to confirm the dysfunction of the visual and visual association cortices in patients with neuropsychologic deficits after DAI.

Individual case-by-case analyses disclosed different distributions of the hypometabolism among the patients. These findings suggest the differences in the regions of brain dysfunction among patients, which may therefore produce different combinations of impaired cognitive domains after DAI. However, the study population in the current study was too small to clarify any correlation between the impaired cognitive domains and the distribution of hypometabolism. Further studies pave the way for systematic analysis between impaired cognitive domains and local neuronal dysfunction of patients after TBI.

Conclusion

By the use of 3D-SSP, an appreciable improvement was achieved in the interpretation of FDG-PET images of the patients after DAI. Local hypometabolism in the cingulate gyrus, lingual gyrus, and cuneus was demonstrated in patients with neuropsychologic deficits after DAI. These results indicate that dysfunction of these cerebral regions plays a key role in neuropsychologic deficits after TBI. This method will allow more comprehensive analyses of the cerebral correlates of neuropsychologic deficits after TBI in the future.

Acknowledgments

We thank S. Fukuyama and Y. Kasuya for technical assistance in this study and S. Uzuyama for assistance in collecting neurobehavioral data. We are indebted to Prof. S. Minoshima for providing the 3D-SSP software and Dr. S. Mizumura for providing the stereotactic extraction estimation software.

References

1. Levin HS, Gary HE, Jr., Eisenberg HM, et al. **Neurobehavioral outcome 1 year after severe head injury: experience of the Traumatic Coma Data Bank.** *J Neurosurg* 1990;73:699–709
2. Ragnarsson KT. **Results of the NIH consensus conference on "rehabilitation of persons with traumatic brain injury."** *Restor Neurol Neurosci* 2002;20:103–08
3. Azouvi P. **Neuroimaging correlates of cognitive and functional outcome after traumatic brain injury.** *Cur Opin Neurol* 2000;13:665–69
4. Ichise M, Chung DG, Wang P, et al. **Technetium-99m-HMPAO SPECT, CT and MRI in the evaluation of patients with chronic traumatic brain injury: A correlation with neuropsychological performance.** *J Nucl Med* 1994;35:217–26
5. Hofman PAM, Stapert SZ, Kroonenburgh MJPG, et al. **MR imaging, single-photon emission CT, and neurocognitive performance after mild traumatic brain injury.** *AJNR Am J Neuroradiol* 2001;22:441–49
6. Stamatakis ME, Wilson JTL, Hadley DM, et al. **SPECT imaging in head injury interpreted with statistical parametric mapping.** *J Nucl Med* 2002;43:476–83
7. Ruff RM, Crouch JA, Tröster AI, et al. **Selected cases of poor outcome following a minor brain trauma: comparing neuropsychological and positron emission tomography assessment.** *Brain Inj* 1994;8:297–308
8. Gross H, Kling A, Henry G, et al. **Local cerebral glucose metabolism in patients with long-term behavioral and cognitive deficits following mild traumatic brain injury.** *J Neuropsychiatry Clin Neurosci* 1996;8:324–34
9. Fontaine A, Azouvi P, Remy P, et al. **Functional anatomy of neuropsychological deficits after severe traumatic brain injury.** *Neurology* 1999;53:1963–68
10. McAllister TW, Sparling MB, Flashman LA, et al. **Neuroimaging findings in mild traumatic brain injury.** *J Clin Exp Neuropsychology* 2001;23:775–91
11. Minoshima S, Koeppe RA, Frey KA, et al. **Stereotactic PET atlas of the human brain: aid for visual interpretation of functional brain images.** *J Nucl Med* 1994;35:949–54
12. Minoshima S, Frey KA, Koeppe RA, et al. **A diagnostic approach in Alzheimer's disease using three-dimensional stereotactic surface projections of fluorine-18-FDG PET.** *J Nucl Med* 1995;36:1238–48
13. Minoshima S, Ficaro EP, Frey KA, et al. **Data extraction from brain PET images using three dimensional stereotactic surface projections.** In: Carson RE, Herscovitch P, Daube-Witherspoon ME, eds. *Quantitative Functional Brain Imaging with Positron Emission Tomography.* San Diego: Academic Press; 1998:133–37
14. Friston KJ, Frith CD, Liddle PF, et al. **The relationship between global and local changes in PET scans.** *J Cereb Blood Flow Metab* 1990;10:458–66
15. Friston KJ, Frith CD, Liddle PF, et al. **Comparing functional (PET) images: The assessment of significant change.** *J Cereb Blood Flow Metab* 1991;11:690–99
16. Minoshima S, Foster NL, Kuhl DE. **Posterior cingulate cortex in Alzheimer's disease.** *Lancet* 1994;24,344:895
17. LeRoux PD, Choudhri H, Andrews BT. **Cerebral concussion and diffuse brain injury.** In: Cooper PR, Golfinos JG, eds. *Head Injury*, 4th ed. New York: McGraw-Hll; 2000:176–94
18. Marshall LF, Eisenberg HM, Jane JA, et al. **A new classification of head injury based on computerized tomography.** *J Neurosurg* 1991;75:S14–S20
19. Minoshima S, Koeppe RA, Frey KA, et al. **Anatomic standaridization: Linear scaling and nonlinear warping of functional brain images.** *J Nucl Med* 1994;35:1528–37

20. Talairach J, Tournoux P. *Co-Planar Stereotactic Atlas of the Human Brain.* New York: Theme Medical Publishers. Inc.; 1998
21. Mizumura S, Kumita S, Cho K, et al. **Development of quantitative analysis method for stereotactic brain image: assessment of reduced accumulation in extent and severity using anatomical segmentation.** *Ann Nucl Med* 2003;17:289–95
22. Lancaster JL, Woldorff MG, Parsons LM, et al. **Automated Talairach Atlas labels for functional brain mapping.** *Human Brain Mapping* 2000;10:120–31
23. Lancaster JL, Rainey LH, Summerlin JL, et al. **Automated labeling of the human brain: a preliminary report on the development and evaluation of a forward-transform method.** *Human Brain Mapping* 1997;5:238–42
24. Kadekaro M, Carne AM, Sokoloff L. **Differential effects of electrical stimulation of sciatic nerve in metabolic actibity in spinal cord and dorsal root ganglion in the rat.** *Proc Natl Acad Sci U S A* 1985;82:6010–13
25. Devinski O, Morrell MJ, Vogt BA. **Contributions of anterior cingulate cortex to behaviour.** *Brain* 1995;118:279–306
26. Fletcher PC, Frith CD, Grabsy PM, et al. **Brain systems for encoding and retrieval of auditory-verbal memory: an in vivo study in humans.** *Brain* 1995;118:401–16
27. Matsunami K, Kawashima T, Satake H. **Mode of [^{14}C] 2-deoxy-D-glucose uptake into retrosplenial cortex and other memory-related structures of the monkey during a delayed response.** *Brain Res Bull* 1989;22:829–38
28. Baleydier C, Mauguiere F. **The duality of the cingulate gyrus in monkey. Neuroanatomical study and functional hypothesis.** *Brain* 1980;103:525–54
29. Finn G, Halligan PW, Marshall JC, et al. **Where in the brain does visual attention select the forest and the trees?** *Nature* 1996;382:626–28
30. Krasnow B, Tamm L, Greicius MD, et al. **Comparison of fMRI activation at 3 and 1.5 T during perceptual, cognitive, and affective processing.** *Neuroimage* 2003;18:813–26
31. Graham DI, Gennarelli TA. **Pathology of brain damage after head injury.** In: Cooper PR, Golfinos JG, eds. *Head Injury*, 4th ed. New York: McGraw-Hill; 2000;176–94
32. Raichle ME, MacLeod AM, Synder AZ, et al. **A default mode of brain function.** *Proc Natl Acad Sci U S A* 2001;98:676–82
33. Greicius MD, Krasnow B, Reiss A, et al. **Functional connectivity in the resting brain: a network analysis of the default mode hypothesis.** *Proc Natl Acad Sci U S A* 2003;100:253–58